Coastal Research Library 42

Carlos Coelho
Caroline Hallin
Francisco Sancho
Paulo A. Silva *Editors*

Coastal Dynamics 2025

Volume 2

OPEN ACCESS

Springer

Coastal Research Library 42

Series Editors

Charles W. Finkl, *Department of Geosciences, Florida Atlantic University, Boca Raton, USA*
Chris Makowski, *Coastal Education & Research Foundation, Inc. (CERF), Charlotte, NC, USA*

The aim of the Coastal Research Library (CRL) is to disseminate accurate information to both the public and research specialists around the world on all aspects of coastal issues in an effort to maintain or improve the quality of our planet's shoreline resources. By covering the entire field of coastal research [e.g., geology, biology, ecology, geomorphology, physical geography, climate change, coastal evolution and shoreline change, littoral oceanography, hydrodynamics and AI modeling, sea-level change, beaches and dunes, coastal hydraulics, erosion, waves, flooding, environmental (resource) management (law), policy and planning, coastal and marine engineering, GIS and remote sensing, socio-economic topics, coastal hazards and extreme storms, anthropogenic change, etc.], the scope of the CRL is broad with a unique cross-disciplinary nature that encompasses all subjects relevant to natural and engineered environments (freshwater, brackish, or marine) and the protection/management of their resources in the vicinity of coastlines around the world. This book series offers current cutting-edge coastal research from the world's leading scientists and is relevant to professionals, academics, and stakeholders, as well as the general public.

The CRL tends to focus on topics linked to complex multidisciplinary problems and contentious issues that surround the coastal environment and occur within the coastal zone. Welcome additions to the series can include: Contributed Volumes, Handbooks, Monographs, Proceedings, Professional Books, Textbooks, and others.

We invite you to submit your new proposals to CRL Series Editor: Chris Makowski, Ph.D. Email: cmakowski@cerf-jcr.com

Carlos Coelho · Caroline Hallin ·
Francisco Sancho · Paulo A. Silva
Editors

Coastal Dynamics 2025

Volume 2

Springer

Editors
Carlos Coelho
Civil Engineering Department
University of Aveiro
Aveiro, Portugal

Caroline Hallin
Water Resources Engineering
Lund University
Lund, Sweden

Francisco Sancho
Hydraulics and Environment Department
National Laboratory for Civil Engineering
Lisbon, Portugal

Paulo A. Silva
Physics Department
University of Aveiro
Aveiro, Portugal

ISSN 2211-0577 ISSN 2211-0585 (electronic)
Coastal Research Library
ISBN 978-3-032-15476-7 ISBN 978-3-032-15477-4 (eBook)
https://doi.org/10.1007/978-3-032-15477-4

This work was supported by the Coastal Dynamics 2025 conference.

This Springer imprint is published by the registered company Springer Nature Switzerland AG
The registered company address is: Gewerbestrasse 11, 6330 Cham, Switzerland

Challenges in Assessing Longshore Transport Along the Gulf of Cadiz Coast: Insights from Analysis of Different Wave Data Sources

Jacqueline Santos[1,2,3](✉), Susana Costas[1], Rui Taborda[2], Juan Garzon[1], and Teresa Drago[2,3]

[1] CIMA/ARNET, University of Algarve, Faro, Portugal
jacsantos@ualg.pt
[2] IDL / FCUL, University of Lisbon, Lisbon, Portugal
[3] IPMA/Portuguese Institute for Sea and Atmosphere, Tavira, Portugal

Abstract. Estimating coastal sediment budgets presents significant challenges due to the complex nature of coastline configurations and the often-bimodal wave regime. This study investigates longshore sediment transport (LST) along the Gulf of Cadiz by analyzing estimates obtained from various wave data sources and employing various approaches. The sensitivity of transport calculations to different wave data sources and approaches is evaluated, and the impact of easterly waves, or "Levante," is examined for the different approaches. The nearshore wave regime was simulated using the SWAN model, with offshore conditions from ERA5 hindcast and the Faro buoy. Results were validated using observational data and LST was estimated using a deep water approximation of the CERC formula, extracting the net transport and the two components of the sediment transport: west-east and east-west. The results emphasize the critical importance of selecting appropriate forcing for applied models to simulate the nearshore wave regime and estimate sediment transport.

Keywords: Longshore sediment transport · Wave data sources · Wave modelling

1 Introduction

Accurate estimations of longshore sediment transport (LST) are essential for understanding coastal dynamics and addressing issues like coastal erosion. LST is primarily influenced by wave parameters, including wave direction, height, and period, which directly control sediment movement along the shoreline. Therefore, analyzing the sensitivity of sediment transport calculations to different wave data sources is important, as variations in wave data can lead to significant differences in transport estimates.

The coast along the Gulf of Cadiz has experienced significant anthropogenic impacts over the past few decades, disturbing the natural sediment transport processes. Coastal infrastructure, dredging, and urbanization have disrupted sediment dynamics, affecting the region's coastal morphology, sediment distribution, and shoreline stability [1]. Some areas along this coast have been the objective of extensive studies, such as the Ria

C. Coelho et al. (Eds.): CD 2025, COASTALRL 42, pp. 84–89, 2026.
https://doi.org/10.1007/978-3-032-15477-4_14

Formosa in southern Portugal. This region has experienced complex shoreline changes, with alternating erosion and accretion trends driven by both natural and human factors with retreat rates as high as 8.96 ± 0.2 m/year [2]. Similarly, the Huelva coast has shown shoreline retreat rates ranging from 10 to 20 m/year [3].

Here, we can come back to the complexity of the coastline and bimodal wave regime. In this context, this study aims to explore different approaches to estimate the potential LST derived from various wave data sources. For that, we focus on evaluating the sensitivity of LST estimates to different wave data sources and on assessing the impact of these variations to model accuracy. Additionally, we investigated the influence of easterly waves, or "*Levante*" on sediment transport.

2 Methods

2.1 Wave Datasets and Propagation

The ERA5 hindcast at coordinates (36.5°N, − 9.0°W) and the Faro buoy data at (36.39°N, -8.06°W) were utilized in both the filtered approach and for resolving the nearshore wave regime. The nearshore wave regime was simulated using the SWAN wave model [4] in non-stationary mode. The model domain extended from 20000 m offshore to 20 m nearshore, with wave parameters extracted at validation sites (Fig. 1). First, a bathymetric grid was generated in QGIS software with available data from two different sources: (i) INGMAR ("*Investigação em Geologia Marinha*"), produced by the National Laboratory of Energy and Geology (LNEG); (iii) REDIAM ("*Rede de Informação Ambiental de Andalucía*"). An unstructured grid was generated using bathymetric of the study area in MATLAB OceanMesh2D tool [5]. The wave spectral domain was discretized into 31 frequency bins and a direction spreading of 36 (10º). Offshore boundary conditions were driven by the wave integral parameters of two different wave data sources: (i) ERA5 hindcast spectra and the Faro buoy (Fig. 1). Wind-wave processes were disabled, and the model was validated against ADCP wave data from two different locations moored c. 20 m depth (Fig. 1). The SWAN model was run for the time interval with observational data (Quarteira: 2020-08-19 to 2021-10-27; Cacela: 2019-07-15 to 2019-10-20).

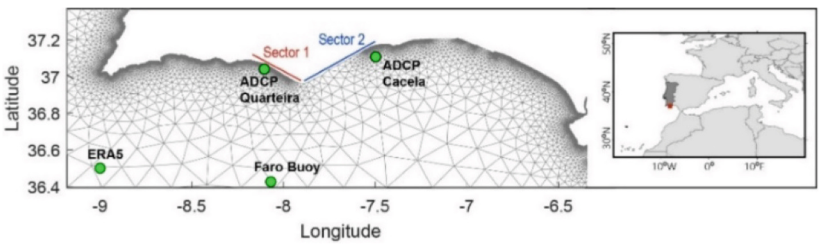

Fig. 1. Gulf of Cadiz showing the location of the two sectors, offshore buoy and wave data point from the ERA5 hindcast model used as boundary conditions (in green), and location of two ADCP moorings used for validation.

Wave data from the ADCP measurements and from SWAN simulations extracted at approximately 20 m (ADCP location) were backpropagated offshore using Snell's law. This procedure allowed the extension of the data to deeper water depths.

In order to better understand sediment transport processes along the Gulf of Cadiz, a simple filtered approach was developed to understand the key factors influencing LST along a coastal stretch exposed to a bimodal wave regime. For that, the wave regime approaching the coast was filtered in order to account only for waves within the direct line-of-sight in relation to a coastal segment (Table 1).

Table 1. Filtered approach settings.

Sector	Location	Representative shoreline orientation	Wave direction filters
1	Quarteira–Ancão	216º	126º–270º
2	Santa Maria Cape–Cacela Velha	145º	90º–235º

2.2 Potential Longshore Sediment Transport

Once all wave data were filtered and backpropagated to deep waters, the potential LST for all wave data sources and approaches was estimated using the CERC formula (Eq. 1) [8]. This approach assumes deep-water waves and a linear, parallel bathymetry. Sediment transport calculations were conducted to determine the net and gross sediment transport for each coastal sector, extracting the corresponding main directional components of sediment transport (w-e and e-w).

$$Qs = K_2 H_{S0}^{\frac{12}{5}} T^{\frac{1}{5}} cos^{\frac{6}{5}}(\theta_{loc}) \sin(\theta_{loc}) \qquad (1)$$

where, the value used for K_2 was 0.497 (calibrated with the ADCP data and assuming an average sediment transport of 1.1×10^5 m^3/year [7]), H_{S0} is the significant wave height offshore (m), T is the peak wave period (s), θloc is the relative angle of wave incidence for waves offshore.

3 Results and Discussion

3.1 Validation of Wave Propagation Scheme

Model performance was assessed by comparing simulated wave parameters (Hs, Tm, and Dir) against observational data from ADCPs (Table 2). Results indicate that the model driven by the Faro Buoy dataset generally outperformed the ERA5-driven model, particularly in terms of wave height (Hs). Using Faro Buoy data as boundary condition produced lower biases and RMS values, along with higher correlation coefficients for Hs and Tm, suggesting better overall agreement with observational data. These findings highlight the sensitivity of the model performance to the choice of boundary condition, with Faro Buoy providing more accurate wave height and period estimations, though both datasets exhibited similar challenges in accurately predicting wave direction.

Table 2. Summary of SWAN model performance compared with ADCP wave data. OBS-Observation data. Model-Boundary condition.

		Bias			RMSE			r		
OBS Data	Boundary conditions	Hs	Tm	Dir	Hs	Tm	Dir	Hs	Tm	Dir
ADCP Quarteira	ERA5	0.21	2.00	−22.68	0.33	4.08	44.96	0.72	0.49	0.29
	Faro Buoy	−0.01	0.90	−4.86	0.24	3.75	33.91	0.78	0.48	0.53
ADCP										
Cacela	ERA5	0.33	−0.24	−36.60	0.42	3.48	55.76	−0.02	0.33	0.17
	Faro Buoy	0.20	−0.45	−16.58	0.29	3.59	42.48	0.51	0.29	0.44

3.2 Potential Longshore Sediment Transport

The results from the analysis of LST in the two sectors show distinct patterns, which depends on both the wave data sources and approach (Table 3). Along the SW-facing Sector 1, the net sediment transport is directed predominantly eastwards, independently of the forcing conditions. The west-east transport often exceeds the east-west (fBUOY-1, fERA5-1 and sERA5-1), implying that this component of the transport dominates clearly. However, for sBUOY-1 and OBS-1, the transport values for both approaches are nearly equal with the net pointing towards the east. In contrast, Sector 2 exhibits lower values for net LST, with some outputs showing predominance in the westward transport (e.g., fBUOY-2 and sERA5-2). This sector is sheltered from higher energy waves approaching from the west, but is exposed to easterly waves, showing lower transport rates with higher variability. A previous study assessed the longshore sediment transport towards the Guadiana ebb-tidal delta, using the CERC2 formula, finding an average rate of 1.9×10^5 m^3/year, and a maximum rate of c. 5.0×10^5 m^3/year, which closely align with the results of the OBS-2 (Table 3).

The direction of longshore sediment transport along the Huelva coast has been reported as eastwards, varying from 50 to 300×10^5 m^3/year [9]. Sediment transport computations based on sBUOY-2 and OBS-2, suggest nearly similar transport in both directions. The results reflect the relative exposure of the coast to a bimodal wave climate, which is dominated by: the W-SW swell generated in the Eastern Atlantic, with "Levante" conditions (short-period waves generated by SE Mediterranean winds) generally playing a secondary role [10, 11].

With regard to the different boundary conditions, both sectors exhibit similar patterns of LST. Specifically, the west-east component consistently exceeds the east-west component for most wave data sources. The LST patterns observed from the sBUOY-1 and sBUOY-2 are closely align with those from the validation OBS-1 and OBS-2 data, suggesting that this approach was more accurate when compared to observational data, in contrast to the other approaches.

Table 3. Longitudinal sediment transport for the sectors (1- Quarteira - Ancão, 2- Santa Maria Cape - Cacela Velha) and different approaches and boundary conditions, including net transport and west-east, east-west components ($\times$ 10^5 m^3/year). The rightmost column shows the relative contribution of easterly waves to transport. OBS-observational data.

Sector	Approach	Boundary condition	Code	W-E	E-W	Net	E (%)
1	Filtered	Faro Buoy	fBUOY-1	30.21	2.95	27.26	9
1	Filtered	ERA5	fERA5-1	21.23	1.20	20.02	5
1	SWAN	Faro Buoy	sBUOY-1	15.21	14.87	0.33	49
1	SWAN	ERA5	sERA5-1	15.24	1.54	13.69	9
1	OBS	-	OBS-1	16.52	15.42	1.10	48
2	Filtered	Faro Buoy	fBUOY-2	0.14	14.27	−14.12	99
2	Filtered	ERA5	fERA5-2	-	-	-	-
2	SWAN	Faro Buoy	sBUOY-2	0.87	0.62	0.25	42
2	SWAN	ERA5	sERA5-2	0.11	0.53	−0.41	82
2	OBS	-	OBS-2	5.23	−3.04	2.18	37

Eastward sediment transport shows significant variability across different approaches and boundary conditions. For most approaches, eastward transport dominates, consistently exceeding 40%. In Sector 1, fBUOY-2 and OBS-2 show eastward transport values of 49% and 48%, respectively. However, there are instances, particularly in Sector 1, where eastward transport is less prominent, with values falling below 9%. In contrast, in Sector 2, eastward transport reaches up to 99% in fBUOY-2.

4 Conclusions

The results from the analysis of LST show distinct patterns, which vary according to both the approach and wave data source in the boundary condition. The results emphasize the critical importance of selecting appropriate wave forcing for applied models to simulate the nearshore wave regime and estimate sediment transport.

Acknowledgements. This work was funded by FCT - Portuguese Foundation for Science and Technology, Ref. 2023.03101, and is a contribution of Coastal Resilience Remote Sensing Monitoring Project funded by FCT - Portuguese Foundation for Science and Technology Reference 2022.05392.PTDC, doi: https://doi.org/https://doi.org/10.54499/2022.05392.PTDC. The authors would like to thank Prof. Paulo Relvas (CCMAR), Dr. Erwan Garel (CIMA) and Dr. Teresa Drago (IPMA) for providing the ADCP data for validation.

References

1. Kombiadou K, Matias M, Ferreira O, Carrasco AR, Costas S, Plomaritis T (2019) Impacts of human interventions on the evolution of the Ria Formosa barrier island system (S. Portugal). Geomorphology **343**:129–144

2. Lira PC, Nobre SA, Taborda R, Andrade C (2016) Coastline evolution of Portuguese low-lying sandy coast in the last 50 years: an integrated approach. Earth Syst. Sci. Data 8(1):265–278
3. Benavente J, Gracia FJ, Del Río L, Anfuso G, Rodríguez-Ramírez A (2015) Caracterización morfodinámica de las playas españolas del Golfo de Cádiz. Bol. Geol. Min. 126(3):409–426
4. Booij N, Ris RC, Holthuijsen LH (1999) A third-generation wave model for coastal regions: 1. Model description and validation. J Geophys Res: Oceans **104**(C4):7649–7666 https://doi.org/10.1029/98JC02622
5. Roberts KJ, Pringle WJ, Westerink JJ (2019) OceanMesh2D 1.0: MATLAB-based software for two-dimensional unstructured mesh generation in coastal ocean modeling. Geoscientific Model Dev **12**(5):1847–1868
6. Santos F, Lopes A, Moniz G, Taborda R, Ramos L (2014) Gestão da Zona Costeira: O Desafio da Mudança. Portuguese Littoral Working Group Report p 237 (in Portuguese)
7. Garel E, López-Ruiz A, Ferreira O (2019) A method to estimate the longshore sediment transport at ebb-tidal deltas based on their volumetric growth: application to the Guadiana (Spain–Portugal border). Earth Surf. Proc. Land. 44(13):2557–2569
8. Ashton AD, Murray AB (2006) High-angle wave instability and emergent shoreline shapes: 1. Modeling of sand waves, flying spits, and capes. J Geophys Res: Earth Surf **111**:1–19
9. CEDEX (2015) Estudio de la dinámica litoral, defensa y propuesta de mejora en las playas con problemas: estudio de actuación del tramo de costa comprendido entre las desembocaduras de los ríos Guadiana y Guadalquivir. Informe final. Madrid p 72 (CEDEX: 22-410-5-001)
10. Ramos J, Gomiz-Pascual JJ, Bruno M (2021) Analysis of wave and wind energy in the Cádiz Gulf coast. In: 14th European Wave and Tidal Energy Conference, 5–9 Sept 2021, pp 1–13
11. Plomaritis TA, Benavente J, Laiz I, Del Río L (2015) Variability in storm climate along the Gulf of Cadiz: the role of large scale atmospheric forcing and implications to coastal hazards. Climate Dyn 45:2499–2514

A New Management Tool to Monitor Salinity Intrusion in the Guadiana Estuary Under Average and Extreme River Discharge Conditions

Guillermo Martín-Llanes[1](✉), Erwan Garel[2], and Alejandro López-Ruiz[1]

[1] Departamento de Ingeniería Aeroespacial y Mecánica de Fluidos, Universidad de Sevilla , Seville, Spain
gmartin1@us.es

[2] Centre for Marine and Environmental Research – CIMA, Universidade do Algarve, Faro, Portugal

Abstract. At the Guadiana Estuary (southern Iberia), strong river flow regulation and the intensification of droughts pose a significant threat to the freshwater resource due to enhanced saltwater intrusion. To accurately predict the salinity dynamics under various river discharge conditions (i.e., average and extreme), a 3-dimensional idealized model (Delft3D) has been developed, calibrated and validated. The overall performances of the model make it a powerful and versatile tool to design and evaluate mitigation management strategies to control salt intrusion during prolonged periods of low river flow. This paper provides a detailed description of the numerical framework and the validation process, together with examples of the future model applications.

Keywords: Salinity · Idealized Modelling · Freshwater Management · Estuary

1 Introduction

Estuaries are amongst the most valuable ecosystems in the world, providing multiple socioeconomic and environmental benefits. These systems are affected by multiple human pressures [1] that alter their hydro-morphodynamics and salinity structure, thus compromising the water quality and the provisioning of ecosystem goods and services. In particular, anthropological activities such as dredging or river regulation promote salinity intrusion, which poses a significant risk for ground and surface freshwater resources.

To control salt intrusion, effective tools need to be developed (1) to assess the vulnerability of estuaries to changes in the salinity field, (2) to predict the impact of future interventions and (3) to design and evaluate mitigation and adaptation solutions to the identified problems. In each of the above cases, the relationship between the estuarine morphology, external forcings and estuarine dynamics must be clearly established [2]. For instance, the control of salt intrusion based on flow regulation requires an advanced knowledge of the salt dynamics in response to a freshwater discharge that can vary by

C. Coelho et al. (Eds.): CD 2025, COASTALRL 42, pp. 382–387, 2026.
https://doi.org/10.1007/978-3-032-15477-4_58

several orders of magnitude at a daily scale. In this context, numerical models, and particularly those based on idealized domains, are considered as efficient tools to obtain primary evaluations and to support management decisions [3].

In this paper, a 3-dimensional idealized model (Delft3D) of the Guadiana Estuary (GE), which river outflow is strongly regulated by dams, was developed to predict the salinity intrusion under varying river flow conditions. The model was calibrated and validated to adequately reproduce the estuary hydrodynamic behavior and the salt transport under low flow conditions, and to simulate the estuary response to transient changes of the river discharge. The provided tool enables to predict the salt intrusion in the estuary and thus to evaluate the efficiency of distinct mitigation strategies.

The document is organized as follows. Section 2 details the model setup (Sect. 2.1) and calibration (Sect. 2.2). The model performances under high and low river flow conditions are presented in Sect. 3. Finally, Sect. 4 outlines various management options proposed by stakeholders to control salt intrusion, which results are currently being evaluated using the model.

2 Numerical Framework

2.1 Model Setup

The physical domain in which the Delft3D numerical model was implemented consists of two parts: (1) the inner shelf, and (2) the channel. The shelf was defined with a constant slope of 0.0025 and seaward extension of 10 km, yielding a maximum depth of 25 m at the offshore boundary. The estuarine channel geometry is idealized, considering a width B(x) which reduces exponentially landward as:

$$B(x) = B_0 exp(-x/b) \quad (1)$$

where B_0 represents the width at the mouth, b represents the convergence length and x indicates the distance along the longitudinal axis, defined from the mouth (x = 0) to the head (x = L). According to the specific geometry of the Guadiana Estuary ([4, 5]), the numerical model was built considering B_0 = 700 m, b = 38 km and L = 78 km.

The cross-channel bathymetry follows a symmetric Gaussian shape [6] which was defined at each section along the cross-channel coordinate y ϵ [−B(x)/2, B(x)/2] by:

$$H(x, y) = H_{thal}(x)\, exp\left(-y^2/2c^2\right) \quad (2)$$

where $H_{thal}(x)$ represents the channel thalweg and varies between H_{thal} = 10 m (at x = 0) and H_{thal} = 9 m (at x = L). The standard deviation (c) was set to 152 to produce a cross-channel average slope of 0.04. To optimize the computational effort and the output files size, the physical domain was divided into three numerical grids using the domain decomposition technique [7], so that the horizontal and vertical resolutions were adapted to adequately simulate the physical processes involved in each region.

The numerical framework and the boundary condition types are shown in Fig. 1. The model is forced by tides and river discharge. The offshore boundary prescribes a harmonic water level condition representing an astronomical tide with 13 harmonics, among which the main is represented by the semidiurnal M_2 component (amplitude = 1 m; phase = 56 º). On the other hand, the freshwater inflow enters the estuary through the upstream section of the river, where a total discharge boundary condition (with uniform vertical distribution of velocities) was established.

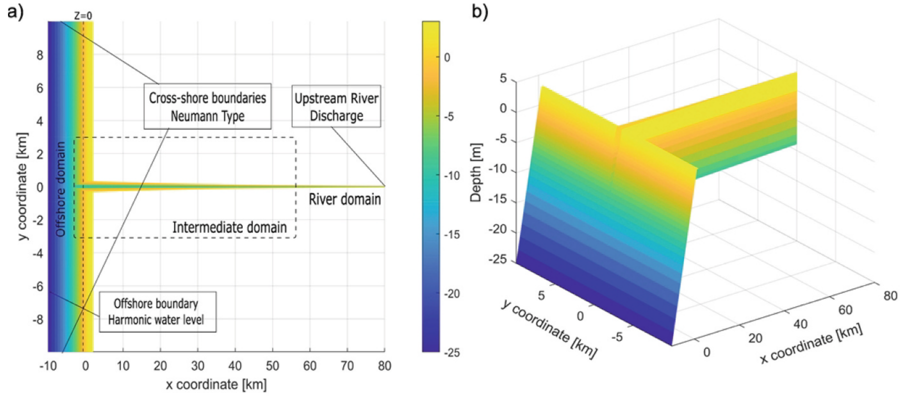

Fig. 1. Numerical model setup: (a) Top view, including boundary conditions and delimitation of subdomains. (b) 3D view of the channel bathymetry and the inner shelf. The color bar indicates depth in meters in a and b.

2.2 Model Calibration and Validation

For calibration, the model was tested considering 12 variants representing different combinations of the roughness coefficient and of the horizontal and vertical eddy viscosities and diffusivities. The performance of each variant was assessed using three different parameters representing the hydrodynamic conditions during distinct periods with low river flow (between 3 and 15 m^3s^{-1}), during which the estuary is well-mixed: (1) the tidal propagation along the estuary [5], (2) the hourly surface salinity near the mouth from March 8 to March 15, 2009 [8], and (3) the depth averaged axial salinity distribution at high water slack, measured at neap (August 31, 2017) and spring (September 8, 2017) tides.

For validation, a high river flow event (March 3 to May 6, 2013, see Fig. 2d for discharge magnitude), was considered to ensure that the model operates correctly under different river flow regimes and adequately reproduces the transient response to high river discharge events. The along channel velocity and salinity simulated during that period were compared with observations near the mouth. The model performance was assessed using the correlation (R) and skill (S) coefficients ([9, 10]).

3 Results: Model Performance

Regarding the low flow conditions analysis, the model configuration giving the best agreement with the field data corresponded to the variant Mod12. The physical parameters in this model configuration are given by a Chezy coefficient of C = 50 $m^{0.5}s^{-1}$, horizontal diffusivity and viscosity of $K_h = A_h = 0.1\ m^2s^{-1}$, vertical diffusivity of $K_v = 2.5{\cdot}10^{-4}\ m^2s^{-1}$ and vertical viscosity of $A_v = 5{\cdot}10^{-4}\ m^2s^{-1}$. With this setup, correlations R of 0.70 and 0.82 were obtained between the computed (15-day average) and measured tidal amplitudes and phases along the channel, respectively (see Fig. 2a, c).

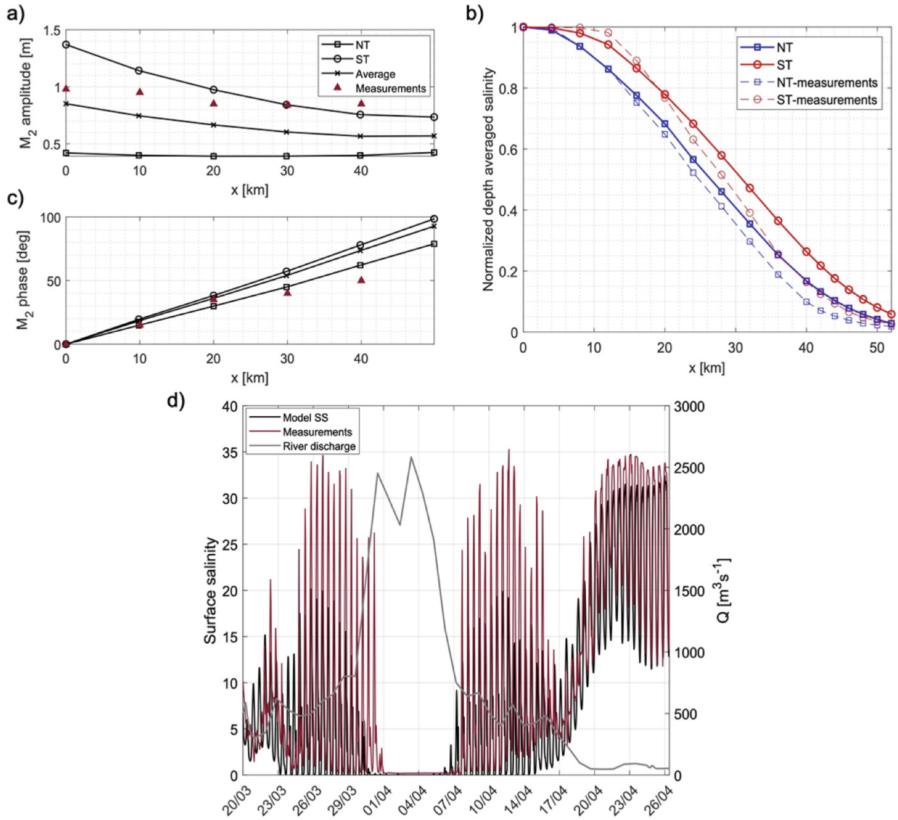

Fig. 2. Model performance. (a) M2 tidal level at neap tide (NT), spring tide (ST) and considering 15-day average (Average). (b) Along-channel depth averaged salinity profiles (high water slack) at neap (NT) and spring (ST) tide. Salinity values are normalized using the seawater salinity. (c) M2 tidal phase at neap tide, spring tide and considering 15-day average regarding symbology from panel (a). (d) Surface salinity near the mouth (left axis) and river discharge (right axis).

Regarding the surface salinity time series, $R = 0.94$ and $S = 0.84$. At high water slack of both neap and spring tides, the coefficients for the depth averaged salinity were $R = 0.94$ and $S = 0.99$, respectively (Fig. 2b). Based on the isohaline of 5 psu (corresponding to a normalized value of 0.14), the predicted intrusion length was 42 km at neap tide and 46 km at spring tide, 4 km more upstream than observed.

Figure 2d represents the salinity at the mouth during the high flow conditions (with river discharge values on the right axis) simulated by the calibrated model. The observations show that the increasing freshwater inflow between March 20 and April 1 steadily reduced the salinity to zero at the time of peak discharge (2500 m^3s^{-1}). The salinity changed from 35 psu to zero in 20 h. Once reached the peak discharge, the estuary remained filled with freshwater for 6 days. After this time, the decreasing discharge led to the resalinization of the estuary, which occurred in two stages: (1) between April 7 and April 16 (when the river flow decreased from 2500 to 500 m^3s^{-1}), and (2) between April 16 to April 20 (when the river flow decreased to 50 m^3s^{-1}). Hence, it took about 2 weeks to recover the salinity values observed before the high discharge event at the mouth.

The model predictions were similar to the above observations. The correlation R was 0.95 for along channel currents and 0.92 for the surface salinity. In particular, the sharp salinity variation in response to the increase in river flow was well reproduced. Likewise, the predicted resalinization period was close to observations. Overall, this validation shows that the model is able to accurately simulate the salinity dynamics in response to transient changes in river flows.

4 Model Application

Through the organization of a workshop with stakeholders, various management scenarios were defined that could impact the salinity intrusion at the GE. These scenarios were organized in four groups of numerical experiments aiming at predicting the salinity distribution after modifications of the bathymetry (Group 1), changes in the river discharge (Group 2), the installation of a freshwater intake station at the upper estuary (Group 3), and various combinations of options from these three groups (Group 4). Group 1 is constituted by three different dredging scenarios: (1) at the lower estuary, (2) at the upper estuary (to allow navigability until the estuary head at Mértola) and (3) throughout the entire channel. Group 2 includes six scenarios with river discharge values varying between 2 and 15 m^3s^{-1}. Group 3 contemplates the pumping of up to 30 hm^3 of freshwater between October and April. Of particular interest, this scenario corresponds to a controversial project which is currently being implemented despite the lack solid scientific evidence backup. The results of these experiments will be presented at the conference.

5 Conclusions

This paper presented the performances of a 3D hydrodynamic model of the GE, represented with an idealized geometry, that requires significantly reduced computational effort compared to more complex numerical models. The results support that the proposed model can successfully predict the salinity dynamics during prolonged periods of low river inflows affected by pulses in the freshwater discharge. Furthermore, the model setup (e.g., bathymetry, inflow or outflow) can be quickly updated with new setup (e.g., bathymetry, freshwater inflow) for the prediction of individual or combined effects of future human interventions – related to freshwater management or not – on the salinity field. In this manner, the model constitutes a useful management support tool for the development and evaluation of mitigation strategies to control salinity intrusion in the estuary.

References

1. Mitchell SB, Jennerjahn TC, Salvatrice V, Zhang W (2015) Changes to processes in estuaries and coastal waters due to intense multiple pressures - An introduction and synthesis. Estuar Coast Shelf Sci 156:1–6
2. Hendrickx GG, Kranenburg WM, Antolínez JA, Huismans Y, Aarninkhof SG, Herman PM (2023) Sensitivity of salt intrusion to estuary-scale changes: a systematic modelling study towards nature-based mitigation measures. Estuar Coast Shelf Sci 295:108564
3. Schuttelaars HM, de Jonge VN, Chernetsky A (2013) Improving the predictive power when modelling physical effects of human interventions in estuarine systems. Ocean Coast Manag 79:70–82
4. Garel E, D'Alimonte D (2017) Continuous river discharge monitoring with bottom-mounted current profilers at narrow tidal estuaries. Cont Shelf Res 133:1–12
5. Garel E, Cai H (2018) Effects of tidal-forcing variations on tidal properties along a narrow convergent estuary. Estuaries Coasts 41:1924–1942
6. Martín-Llanes G, López-Ruiz A (2024) The role of estuarine convergence on the salinity distribution and the estuary response to short river discharge pulses. Estuar Coast Shelf Sci 306:108893
7. Deltares (2016) Delft3D-FLOW: User manual (3.15)
8. Garel E, Ferreira Ó (2015) Multi-year high-frequency physical and environmental observations at the Guadiana Estuary. Earth Syst. Sci. Data 7:299–309
9. Willmott CJ (1981) On the validation of models. Phys Geogr 2:184–194
10. Zarzuelo C, López-Ruiz A, Ortega-Sánchez M (2021) The role of waves and heat exchange in the hydrodynamics of multi-basin bays: the example of Cádiz Bay (Southern Spain). J Geophys Res Oceans 126